The University of Maine
DigitalCommons@UMaine

Earth Science Faculty Scholarship

Earth Sciences

3-27-2009

Along-Strike Differences in the Southern Alps of New Zealand: Consequences of Inherited Variation in Rheology

Phaedra Upton

Peter O. Koons
University of Maine - Main, peter.koons@maine.edu

Dave Craw

C. Mark Henderson

Ray Enlow

Follow this and additional works at: https://digitalcommons.library.umaine.edu/ers_facpub

Part of the Earth Sciences Commons

Along-strike differences in the Southern Alps of New Zealand: Consequences of inherited variation in rheology

Phaedra Upton,[1,2,3] Peter O. Koons,[1] Dave Craw,[2] C. Mark Henderson,[4] and Ray Enlow[5]

[1] Long- and short-term strain variations along the Australian-Pacific plate boundary through the South Island of New Zealand, including a 300% increase in orogen width, coexistence of oblique thrusting on orthogonal structures, and variability in the locus of orogenic gold deposits, coincide with rheologically relevant geological variation. Our model investigates the consequences of thin, strong lower crust in the north and thick, weak lower crust in the south. Solution of the full 3-D mechanical equations reproduces the larger wavelength strain patterns of the orogen. A 3-D perturbation-based analytical solution leads to the identification of the sensitivity of displacement type to minor stress changes. Transition from boundary-normal thrusting to boundary-parallel thrusting occurs at the transition from strong to weak lower crust and is related to an increase in either τ_{yz} (shear stress in the yz plane) or the ratio of the coordinate normal stresses, (σ_{yy}/σ_{xx}), where x and y are in the horizontal and z is vertical. Both mechanisms are compatible with the geologically dependent rheological variation employed in our model. **Citation:** Upton, P., P. O. Koons, D. Craw, C. M. Henderson, and R. Enlow (2009), Along-strike differences in the Southern Alps of New Zealand: Consequences of inherited variation in rheology, *Tectonics*, *28*, TC2007, doi:10.1029/2008TC002353.

1. Introduction

[2] The Southern Alps of New Zealand are a highly three-dimensional mountain range and yet have generally been described using two-dimensional cross-sectional models [e.g., *Wellman*, 1979; *Koons*, 1990; *Beaumont et al.*, 1992; *Willett et al.*, 1993; *Upton*, 1998; *Koons et al.*, 2003]. These models are insufficient to describe deformation fields resulting from oblique plate motions and/or spatially variable rheological behavior and boundary conditions [*Gerbault et al.*, 2003; *Upton and Koons*, 2007]. Several examples

of plate boundary parallel variation exist in the Southern Alps, including significant orogen width variation (Figure 1a), variation in orientation of principal horizontal strain axes, the existence of a region of anomalous displacement partitioning (coeval thrusts oriented parallel and perpendicular to the plate boundary), an increase in crustal thickness from north to south (Figure 1c) and changes in the location of the locus of fluid flow and orogenic gold deposition (*Craw et al.*, 2007). We suggest that the increase in crustal thickness from north to south, and an associated variation in lower crustal strength, leads to the other characteristics mentioned and in this study we use numerical and analytical calculations to test this theory. By comparing strain and displacement fields from three-dimensional models with surface, geochemical and geophysical observations, we can impose bounds upon the dynamics compatible with real systems.

[3] Within the framework of our three-dimensional numerical models, conditioned by the geometry and far-field plate driving forces of the South Island, we investigate the influence lower crustal strength and thickness has on the nature of the developing orogen. The horizontal distribution of strain within a zone of oblique convergence reflects tectonic boundary conditions as transmitted through the rheological structure of the deforming lithosphere. In this case the crust that we are considering is thin and strong in one region and weak and thick in another.

[4] We also present an analytical approximation of our rheological model which uses perturbation theory to determine whether or not our model can produce the distinctive displacement partitioning observed in the eastern Southern Alps (Figure 1a). This method has previously been described by *Enlow and Koons* [1998] and used by *Upton et al.* [2008].

2. Southern Alps of New Zealand

2.1. Tectonic Setting

[5] The microcontinent Zealandia, of which New Zealand is the subaerial portion, was largely formed off the edge of Gondwana in the Mesozoic [*Wandres and Bradshaw*, 2005]. A distinct plate boundary began to develop through Zealandia at circa 45 Ma [*Sutherland*, 1999]. Since that time, 850 km of dextral shear is inferred to have occurred across the South Island [*Sutherland*, 1999]; 460 km of dextral strike slip is evident along the present-day plate boundary, the Alpine Fault, an oblique reverse structure which dips SE beneath the Southern Alps [*Norris et al.*, 1990]. The remaining 400 km have been taken up by distributed shear across the South Island [*Coombs et al.*, 1976; *Molnar et al.*, 1999; *Cox and Sutherland*, 2007]. Today, the relative far-field plate vector driving fault movement and associated deformation is directed

---

[1]Department of Earth Sciences, University of Maine, Orono, Maine, USA.
[2]Geology Department, University of Otago, Dunedin, New Zealand.
[3]Now at GNS Science, Dunedin, New Zealand.
[4]Department of Geological Sciences, Victoria University, Wellington, New Zealand.
[5]Department of Mathematics and Statistics, University of Otago, Dunedin, New Zealand.
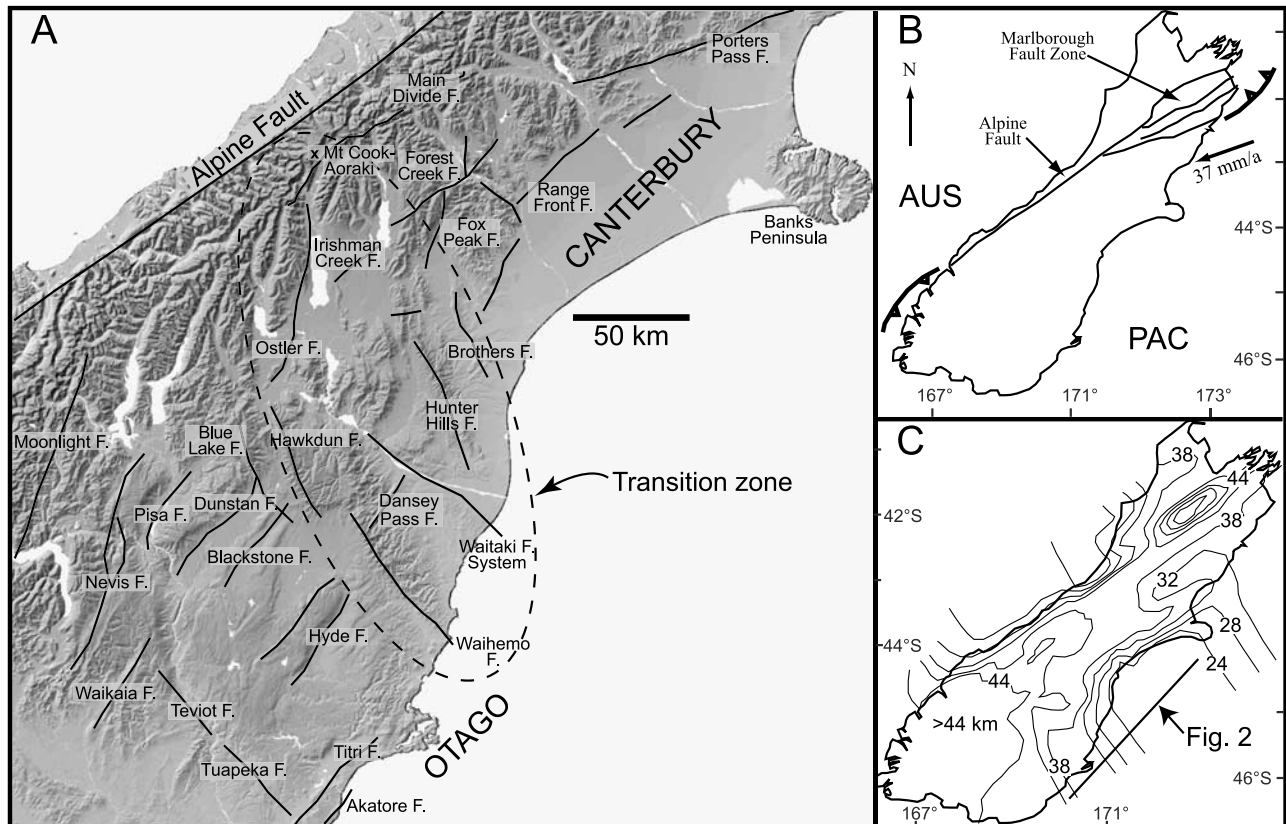
Figure 1. (a) DEM of southern South Island of New Zealand showing active fault traces. Note the difference in width of the orogen from Canterbury southwest to Otago. (b) Regional tectonics of the South Island. The plate motion vector is shown relative to a fixed Australian plate (modified NUVEL-1A solution of *DeMets et al.* [1994]). PAC, Pacific plate; AUS, Australian plate. (c) Estimates of crustal thickness from the isovelocity curve corresponding to 7.8 km s^{-1} (velocity data from *Eberhart-Phillips and Reyners* [1997, 2001] and *Eberhart-Phillips and Bannister* [2002], modified from *Kohler and Eberhart-Phillips* [2003]).

ENE-WSW with relative motion of ∼37 mm a^{-1} [*DeMets et al.*, 1994], resolved into 35.5 mm a^{-1} parallel to the plate boundary and 10 mm a^{-1} perpendicular, in the central South Island. Estimates of exhumation rates are on the order of 6–9 mm a^{-1} [*Wellman*, 1979; *Simpson et al.*, 1994; *Norris and Cooper*, 2001; *Little et al.*, 2005] in the central Southern Alps, immediately adjacent to the Alpine Fault and decrease eastward to ∼1 mm a^{-1} or less east of the Main Divide [*Blick et al.*, 1985]. Uplift rates adjacent to the Alpine Fault decrease to 5–6 mm a^{-1} to the northeast, as much of the relative motion is transferred to the Hope Fault [*Norris and Cooper*, 2001]. South of Hasst, uplift rates decrease to ∼3 mm a^{-1} as motion is partitioned into the Fiordland subduction zone [*Norris and Cooper*, 2001].

[6] To the north and south of the central South Island the tectonics of Zealandia reflect the changing character of the Australian-Pacific plate boundary in the south Pacific (Figure 1b). To the north, the oceanic Pacific plate subducts beneath the Australian plate and to the south, the oceanic Australian plate is obliquely overridden by the Pacific plate. The South Island of New Zealand is dominated by the actively rising Southern Alps along the continent-continent

portion of the plate boundary (Figure 1a). Transition from continental collision to subduction occurs across the Northern South Island. Here five major dextral slip faults strike at a low angle to the present Australia-Pacific plate convergence vector. These are known as the Marlborough Fault Zone, and their strike-slip motion accommodates most of the plate motion with underthrusting of the Pacific plate and uplift and shortening within the Australian crust taking up most of the rest. The Marlborough faults young to the south, with the oldest and westernmost, the Wairau Fault, exhibiting the greatest total offset [*Little and Jones*, 1998]. To the south of the central Southern Alps, the Alpine Fault steepens and becomes dominantly strike-slip as relative plate motion is partitioned onto a series of offshore thrust faults which link into the northern end of the Puysegur Trench [*Barnes et al.*, 2005].

2.2. Three-Dimensional Nature of the Orogen

[7] Oblique collision between the Australian and Pacific plates in the South Island of New Zealand is often treated as varying only in the direction normal to the plate boundary, the Alpine Fault [e.g., *Wellman*, 1979; *Koons*, 1990; *Beaumont et al.*, 1992; *Willett et al.*, 1993; *Upton*, 1998]. Two-dimensional

cross sections through the central South Island, normal to the Alpine Fault, have commonly been used to represent the mechanical behavior of the oblique convergence in either two-dimensional [e.g., *Koons*, 1990; *Beaumont et al.*, 1992; *Willett et al.*, 1993; *Upton*, 1998], or three-dimensional formulations [e.g., *Koons*, 1994; *Koons et al.*, 1998]. In reality, the width and character of the zone of active deformation associated with oblique collision varies significantly along strike of the plate boundary (Figure 1a) as mentioned in previous geodynamic descriptions [*Gerbault et al.*, 2003; *Upton and Koons*, 2007]. To the south of the central Southern Alps, the zone of modern deformation widens by ∼100%, the basement geology is dominated by midcrustal schists as opposed to graywacke and an orthogonal pattern of actively growing ranges dominates the topography of the transition zone (Figure 1a). Consequently, a single cross-sectional view of the South Island provides an incomplete representation of the deformation along this portion of the plate boundary.

2.3. Canterbury and Otago Strain Regimes

[8] The regions we consider in this study are within the central and southern South Island, which lie to the south of the Marlborough Fault System, and are known by the regional names Canterbury and Otago, respectively (Figure 1). The eastward extent of modern deformation associated with oblique Australian-Pacific collision can be broadly correlated with the width of elevated topography in the South Island. In the Canterbury region, which extends for ∼100 km along strike, from the Porter's Pass Fault south to the Hunter Hills and Brothers faults, the Southern Alps are narrow, ∼70 km wide, reflecting deformation concentrated close to the plate boundary and strain rates on the order of $5 \times 10^{-7} a^{-1}$ [*Beavan et al.*, 1999, 2007; *Henderson*, 2003] (Figure 1a). The topography northwest of the Porter's Pass Fault is associated with the Marlborough Fault System. Note also that the topography east of this region, Banks Peninsula, is volcanic in origin, dated at ∼8−11 Ma [*Sewell*, 1988] and is not associated with the present-day collision. In Otago and South Canterbury, deformation associated with the current tectonic regime extends ∼200 km to the east coast, including the Southern Alps and the Central Otago Ranges, in a broad zone of lower strain rates (<$5 \times 10^{-8} a^{-1}$ (P. Denys, personal communication, 2008)) and distributed deformation (Figure 1a).

[9] Active deformation in central Canterbury is dominated by oblique reverse faulting with minor folding. Structures predominately fall into two distinct patterns: those oriented NE, parallel to the Alpine Fault, and those oriented north (Figure 1). The first category includes the Forest Creek faults, Irishman Creek faults, the Range Front faults and the now inactive Main Divide Fault Zone [*Cox and Findlay*, 1995; *Upton et al.*, 2003a, 2004]. The second category includes the Ostler Fault [*Blick et al.*, 1989; *Ghisetti et al.*, 2007; *Amos et al.*, 2007] and the Fox Peak faults [*James*, 1998; *Upton et al.*, 2003a, 2004]. Minor folding is associated with the Fox Peak faults [*James*, 1998; *Upton et al.*, 2003a, 2004]. Active deformation in Otago occurs on NE trending folds and faults such as the Hyde, Dunstan, Blackstone, and Pisa faults. The folds in this area have been shown to be active fault propagation folds [*Markley and Norris*, 1999; *Jackson et al.*, 1996].

[10] The region between Canterbury and Otago is characterized by the coexistence of orthogonal thrust faults striking NE and NW (Figure 1a). Note these are not conjugate thrust faults which would be parallel but oppositely dipping but are orthogonal with transport directions at 90 degrees to one another. The NW striking faults are the Waihemo/Hawkdun faults and Waitaki Fault System; both are associated with normal faults formed during Cretaceous extension [*Laird*, 1993; *Sutherland et al.*, 2001]. The NE striking faults include the Dansey Pass Fault and other parallel unnamed faults [*Forsyth*, 2002]. Both NE and NW striking fault sets are active implying a stress regime in which σ_1 and σ_2 (maximum and intermediate principal stresses) are close and easily switched [*Enlow and Koons*, 1998].

[11] Another apparent anomaly exists in the transition between Canterbury and Otago. Some faults in this region exhibit sinistral strike-slip motion, kinematics rare in New Zealand which is dominated by dextral deformation. For example, a late Quaternary fault trace along the Wharekuri Fault in the Waitaki Valley records sinistral strike-slip motion [*Gair and Gregg*, 1960; *Forsyth*, 2002] (Figure 2a). Likewise, post-Pliocene offset on the Ostler at the edge of the mountains along the Canterbury-Otago transition is sinistral [*Templeton et al.*, 1999] (Figure 2a).

2.4. Basement Geology

[12] The basement for the Southern Alps consists of metasedimentary terranes that were amalgamated along the Gondwana margin in the Mesozoic [*MacKinnon*, 1983; *Norris and Craw*, 1987; *Mortimer*, 1993a, 1993b] (Figure 2c). The Gondwana margin was oriented approximately south southeast [*Wandres and Bradshaw*, 2005]. Accounting for Cenozoic rotations, it was parallel to the present-day boundary between Canterbury and Otago and was orthogonal to the present-day plate boundary (Figure 2c). The Torlesse Terrane is the most significant of these terranes as it underlies both Canterbury and Otago [*MacKinnon*, 1983; *Mortimer*, 1993a, 1993b]. The Canterbury portion of this terrane is an accretionary complex made up of variably deformed quartzofeldspathic metagraywackes [*MacKinnon*, 1983]. Exposed Torlesse rocks are dominated by unfoliated graywackes (prehnite-pumpellyite facies), with some kilometer-scale slices of weakly foliated schists (pumpellyite-actinolite facies) (Figures 2a and 2b). Jurassic collision between the Torlesse Terrane and the Aspiring and Caples terranes resulted in the thick metamorphic pile that became the Otago crustal block [*Norris and Craw*, 1987; *Mortimer*, 1993a, 1993b]. The metamorphic belt was unroofed erosionally and tectonically between the Jurassic and middle Cretaceous, exposing greenschist facies rocks (up to biotite-garnet zone) over most of Otago (Figures 2a and 2b) [*Craw*, 1998; *Mortimer*, 2000].

[13] Extensional deformation in the middle Cretaceous resulted in steep and gently dipping normal faulting, oriented NE and NW, especially along the margins of the Otago schist belt where 1−5 km scale rock slices of differing metamorphic grades were juxtaposed [*Deckert et al.*, 2003; *Gray and Foster*,
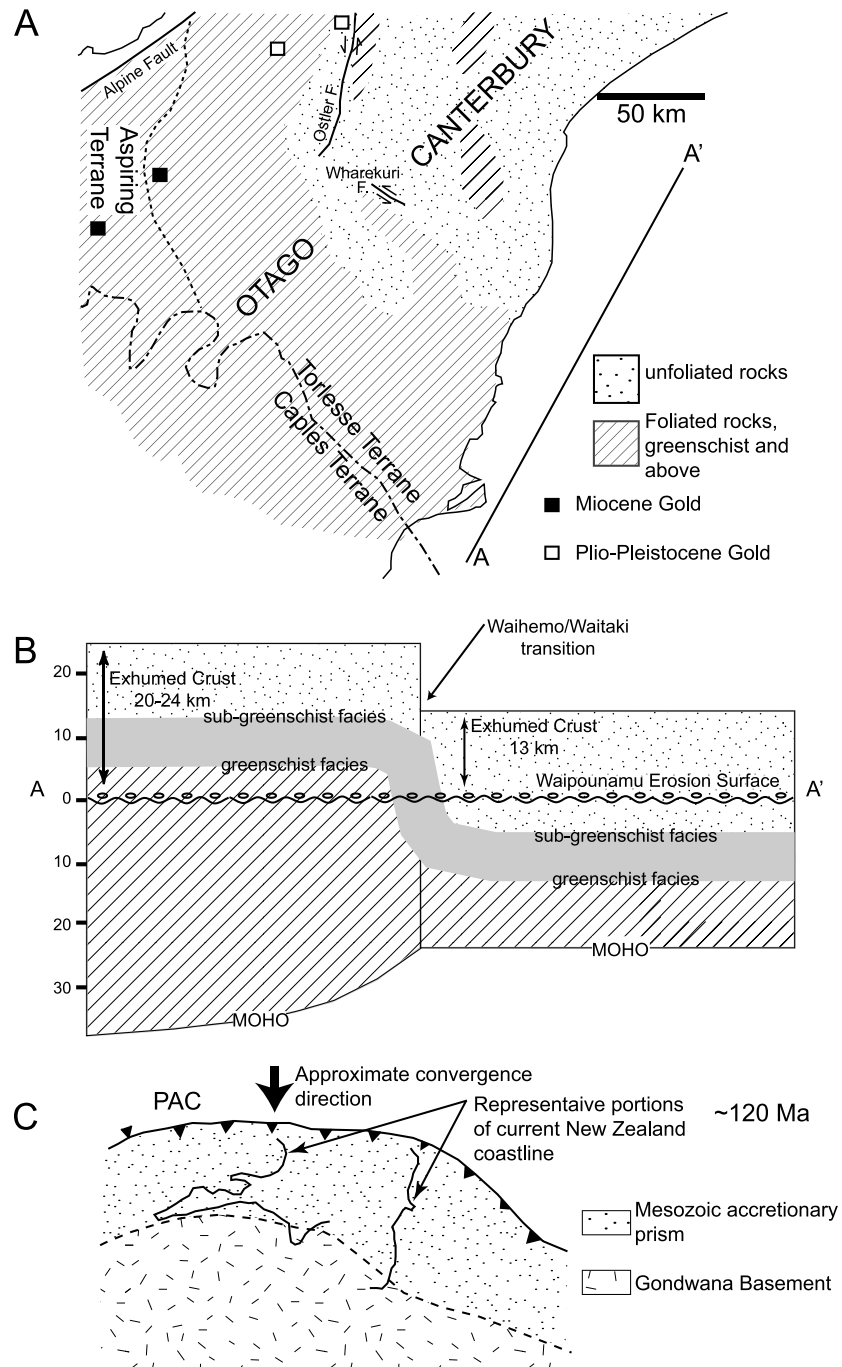
Figure 2. (a) Geological map showing elements discussed in the text including the transition between foliated (schist) and unfoliated (graywacke) rocks, the Torlesse-Caples boundary, localities of Miocene and Plio-Pliestocene gold deposits, and sinistral strike-slip faults. (b) Schematic cross section (location shown in Figure 1c) showing the present-day crustal thickness and amount of material exhumed from Otago and from Canterbury. Wavy line represents the Waipounamu erosion surface [*Landis et al.*, 2008]. (c) Simplified reconstruction showing the geology of the New Zealand region at ~120 Ma (modified from *Wandres and Bradshaw* [2005] with permission).

2004; *Craw et al.*, 2007]. Extension continued, accompanying the breakup of Gondwana, through to the Oligocene when Zealandia was essentially submerged below sea level [*Landis et al.*, 2008]. Marine planation accompanied this progressive submergence, leading to a widespread diachronous unconformity, the Waipounamu erosion surface (Figures 2a and 2b), that cut into the basement rocks and remnants of Cretaceous– early Tertiary sediments [*LeMasurier and Landis*, 1996;

Landis et al., 2008]. Zealandia reemerged from the sea, beginning in the late Oligocene–early Miocene, with the development of the current Pacific-Australian plate boundary through the region [*Sutherland*, 1999]. Deeper levels (greenschist facies and amphibolite facies) of the Canterbury portion of the Torlesse Terrane are now being exposed by Southern Alps uplift and exhumation immediately SE of the Alpine Fault (Figure 1a). Maximum uplift, maximum exhumation and highest relief are all focused near Mount Cook–Aoraki (Figure 1a).

2.5. Crustal Thickness

[14] Present-day crustal thickness varies both along and across the South Island (Figure 1c). A crustal root has developed along the central South Island, associated with the present-day continental collision. This crustal root reaches depths of ∼44 km beneath western Otago [*Scherwath et al.*, 2003; *Melhuish et al.*, 2005; *Bourguignon et al.*, 2007]. In this study, we are interested in the initial thickness of the Canterbury and Otago regions, prior to the start of Cenozoic collision. The best estimate we have for precollisional thicknesses is the present-day crustal thickness at the eastern edge of the continent, which appears to be unaffected by the present-day mountain building. Estimates of Moho depths in mid-Canterbury derived from seismic reflection (SIGHT transect 1), refraction and inversion of seismic velocities are 18 km in the Bounty Trough and ∼25 km at the East Coast [*Van Avendonk et al.*, 2004]. Sixty kilometers to the southwest, along SIGHT transect 2, Moho depth is estimated at ∼27 km at the East Coast [*Scherwath et al.*, 2003]. The Moho deepens parallel to the coast to ∼32 km east of Otago [*Kohler and Eberhart-Phillips*, 2003]. Further evidence comes from velocity inversion which suggests that lower crustal rocks extend an additional 10 km downward in Otago relative to Canterbury [*Eberhart-Phillips and Bannister*, 2002; *Stern et al.*, 2001].

[15] The pre-Cenozoic Otago crust was thicker than that in Canterbury as a result of collision between quartzofelspathic graywackes of the Torlesse Terrane and arc-derived graywackes of the Caples terranes on the eastern edge of Gondwana [*Mortimer*, 1993a, 1993b; *Bradshaw*, 1989; *Gray and Foster*, 2004]. The rocks to the north of Otago were not thickened by the Mesozoic collision. The bulk of the metamorphism and deformation associated with collision occurred between ∼160 and 140 Ma through to 120 Ma [*Gray and Foster*, 2004]. This was followed by very slow exhumation and cooling until ∼110 Ma and more significant exhumation of the high-grade metamorphic core between 109 and 100 Ma [*Gray and Foster*, 2004]. During this time the crust underlying what is now Canterbury was further from the Mesozoic collision zone, closer to the subduction margin and underwent little if any deformation [*Bradshaw*, 1989] (Figure 2c).

3. Mechanical Modeling

3.1. Mechanical Models

[16] We model the oblique deformation that occurs along the South Island transpressional boundary using a two-
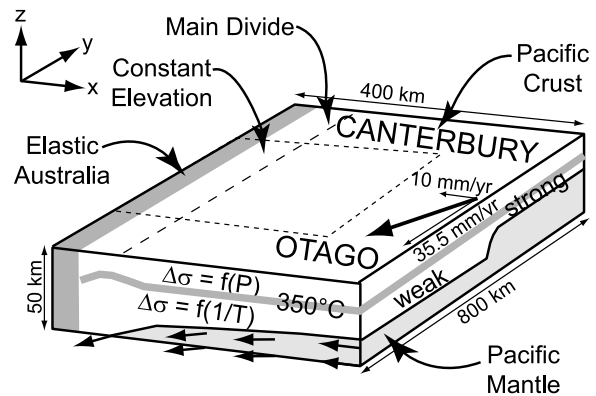

Figure 3. Geometry and boundary conditions for the three-dimensional mechanical model. Model is of a two-layered crust which is subjected to oblique compression. Material is pushed from the right and dragged along the base at velocities of 35.5 mm a^{-1} parallel to (along y axis) and 10 mm a^{-1} normal to (along x axis) the plate boundary. Crustal rheology is approximately horizontal; the upper crust is represented by a pressure-dependent rheology, and the lower crust and mantle is represented by a temperature-dependent rheology. The model has an along-strike variation with the lower crustal material of the Otago region being considerably weaker than the lower crustal material of the Canterbury region. Approximately steady state elevations are maintained adjacent to the plate boundary. Axes define reference frame used where y is parallel to the plate boundary and x is normal to the plate boundary. Dashed box is the approximate region of the model results shown in Figures 5 and 7.

layered crust overlying an elastic Pacific mantle (Figure 3). The solution domain is a three-dimensional numerical region extending 400 km normal to the plate boundary (x) by 800 km parallel to the plate boundary (y) by 50 km depth (z). The western edge of the model consists of an elastic block simulating the Australian plate which deforms minimally. The erosional regime of the Southern Alps is a result of a strongly asymmetric precipitation pattern that efficiently removes material from the western inboard slope [*Koons*, 1990; *Beaumont et al.*, 1992; *Willett et al.*, 1993]. We have simulated this orographic effect by maintaining the western slope at a constant elevation [*Koons et al.*, 1998, 2003; *Upton and Koons*, 2007].

[17] Our models are aimed at unraveling crustal deformation and the displacement of the mantle is imposed as a boundary condition. Previously, two end-member kinematic models have been used to explain strain accommodation within the mantle lithosphere beneath the Southern Alps. One model evokes South Island subcrustal mantle deformation over >200 km [*Molnar et al.*, 1999; *Moore et al.*, 2002; *Baldock and Stern*, 2005], while the other model assumes little or no deformation in the uppermost mantle and resembles a subduction type boundary condition [e.g., *Beaumont et al.*, 1992; *Koons et al.*, 2003; *Ellis et al.*, 2006; *Upton and Koons*, 2007]. We have chosen a subduction boundary

condition where the Pacific plate is descending beneath the Australian plate without a large region of mantle deformation, based on a comparison between mechanical models and observations [e.g., *Ellis et al.*, 2006; *Liu and Bird*, 2006; *Savage et al.*, 2007; *Beavan et al.*, 2007; *Upton and Koons*, 2007]. These boundary conditions are similar to previously published mechanical models of the Southern Alps [*Koons et al.*, 1998, 2003; *Upton and Koons*, 2007]. The two-layered Pacific crust is dragged along its base, 25 km below sea level for Canterbury and 35 km below sea level for Otago, at a velocity of 35.5 mm a^{-1} parallel to (along y axis) and 10 mm a^{-1} normal to (along x axis) the plate boundary compatible with the calculated relative plate vectors from NUVEL-1A [*DeMets et al.*, 1994] (Figure 1b). The northwestern edge of the model, representing the Australian plate, is held fixed. The velocity conditions on the lateral boundaries are allowed to vary through the model time. We do this by taking the velocity profiles from $y = \pm 300$ km (internal to the model) and imposing those velocity condition on the lateral boundaries, that is $y = \pm 400$ km. These boundary conditions are continually updated as the model runs. This method allows these oblique boundaries to develop as a function of the rheology. Note that Figures 5 and 7 only show the central portion of the models, the solution domain, and do not extend out as far as the lateral boundaries.

3.2. Solution Methodology

[18] Models were developed using the numerical code FLAC^{3D} a three-dimensional finite difference code, which we have modified to accommodate large strains and local erosion [*Cundall and Board*, 1988]. A large number of comparisons have been made between FLAC^{3D} results and exact solutions for plasticity problems (ITASCA, FLAC^{3D} (Fast Lagrangian Analysis of Continua in 3 Dimensions, 1997, available at http://www.itascacg.com/flac3d/index.php). The results show uniformly good agreement with theoretical solutions and in modeling geometrical instabilities well past the collapse or failure limit. Materials are represented by polyhedral elements within a three-dimensional grid that uses an explicit, time-marching solution scheme and a form of dynamic relaxation. Each element behaves according to a prescribed linear or nonlinear stress/strain law in response to applied forces or boundary restraints. The inertial terms in Cauchy's equations of motion

$$\frac{\partial \sigma_{ij}}{\partial x_i} + \rho b_i = \rho \frac{dv_i}{dt} \qquad (1)$$

(where σ_{ij} is the stress tensor, x_i, v_i are the vector components of position and velocity, respectively, ρ is the density of the material, and b_i is the body force) are used as a numerical means to reach the equilibrium state of the system under consideration. The resulting system of ordinary differential equations is then solved numerically using an explicit finite difference approach in time. The drawbacks of the explicit formulation (i.e., small time step limitation and the question of required damping) are overcome by automatic inertia scaling and automatic damping that does not influence the mode of failure. The governing differential equations are solved alternately, with the output for the solutions of the equations of motion used as input to the constitutive equations for a progressive calculation. Solution is achieved by approximating first-order space and time derivatives of a variable using finite differences, assuming linear variations of the variable over finite space and time intervals, respectively. The continuous medium is replaced by a discrete equivalent with all forces involved concentrated at the nodes of a three-dimensional mesh used in the medium representation.

3.3. Model Crustal Rheology

[19] Numerical modeling requires approximating the rheology of the material being studied by a mathematical description of the stress/strain or stress/strain rate relationship. The rheological descriptions we use are generally derived from laboratory experiments. Crustal rheology is unlikely to be as simple as these experimentally derived flow laws would imply, however, a sharp reduction in flow stress at temperatures above 300–350°C due to the exponential dependence upon temperature appears to be a robust feature of quartz- and feldspar-dominated crust [*Sibson*, 1982]. We have chosen a rheological model similar to the "jelly sandwich" type [*Chen and Molnar*, 1983; *Burov and Watts*, 2006].

[20] Crustal velocities of 6.0–6.2 km s^{-1} determined for the upper and midcrust of the Southern Alps along SIGHT transects 1 and 2 are compatible with a quartzofeldsapthic dominated crust [*Scherwath et al.*, 2003; *Van Avendonk et al.*, 2004]. At the base of the crust, crustal velocities of 7.0–7.1 km s^{-1} are consistent with a more mafic rheology [*Scherwath et al.*, 2003; *Van Avendonk et al.*, 2004]. Given these values, we represent crustal materials using an elastic/Mohr-Coulomb, pressure-dependent upper crust overlying an elastic/Von Mises middle and lower crust with flow parameters determined from the published creep laws at a reference strain rate of 10^{-14} s^{-1} and an average geothermal gradient of 20°C km^{-1} (equation (2)) [e.g., *Upton and Koons*, 2007]:

$$K_\varphi = 0.5 \Delta\sigma \qquad (2)$$

where

$$\Delta\sigma = \left[\left(\frac{\dot{\varepsilon}}{A} \right) \exp\left(\frac{Q}{RT} \right) \right]^{1/n},$$

$\Delta\sigma$ differential stress, $\sigma_1 - \sigma_3$;
K_φ shear strength of the material;
A a preexponential factor;
$\dot{\varepsilon}$ shear strain rate;
n power law exponent;
Q activation energy;
R universal gas constant;
T temperature (K).

Table 1. Parameters, Material Properties, and Initial Conditions Used in the Numerical Models

	Region	
	Canterbury	Otago
Bulk modulus (Pa)	1×10^{10}	1×10^{10}
Shear modulus (Pa)	3×10^{9}	3×10^{9}
Density (kg m^{-3})	2800	2800
Friction angle (deg)	35	35
K_{σ}	1×10^{6} to 1×10^{8}	1×10^{5} to 6×10^{7}

[21] We approximate temperature-dependent weakening by decreasing the value of K_{φ} with increasing temperature in a manner constant with yield stress data for rheologies determined by laboratory creep experiments. A, Q, and n are determined from extrapolation of experiments on wet synthetic quartzite [*Paterson and Luan*, 1990]. $A = 6.5 \times 10^{-8}$ MPa^{-n} s^{-1}; $Q = 135$ kJ mol^{-1}; $n = 3.1$. In the lower crust the rheology is dominated by mafic minerals [*Scherwath et al.*, 2003; *Van Avendonk et al.*, 2004]. We use the diabase rheology of *Shelton and Tullis* [1981] as an estimate for lower crustal strength, $A = 2 \times 10^{-4}$ MPa^{-n} s^{-1}; $Q = 260$ kJ mol^{-1}; $n = 3.4$ (Table 1).

[22] We have defined the lower crust in this way rather than using the power law rheology also available to us in FLAC^{3D} as we have found that our solutions are more stable when running to higher strains. We recognize that we are unable to model time-dependent behavior or localization using this definition. The reference strain rate of 10^{-14} s^{-1} is likely to be too low for materials close to the Alpine Fault, but the scale of our models is such that we cannot localize deformation to the extent that occurs in nature. In the central Southern Alps (adjacent to the Canterbury region), ~75% of strain is focused onto the Alpine Fault at the surface [*Norris and Cooper*, 2001]. This leaves ~25% distributed across the rest of the orogen. We are using a large-scale model, with a resolution of 4 km per grid cell, across the >200 km width of the orogen. Our analysis is concentrated on the lower strain eastern portion of the orogen, and for these reasons, we feel that this simplifying assumption can be justified.

[23] The rheological properties are varied along strike of the boundary in a manner constrained by the geological arguments presented above (Figure 4). The northern half of the model represents the Canterbury region, the crust here is given a thickness of 25 km and the lower crust is strong (Figures 3 and 4). The southern half of the model represents the Otago region. It is given a crustal thickness of 35 km and the lower crust is weak relative to that of the Canterbury region (Figures 3 and 4).

[24] It is the relative difference in the strengths that is important for the modeling rather than the details of the actual values. Thus we believe that using an approximation based on a quartzite upper crust and a diabase lower crust for different crustal thicknesses is reasonable. The difference in strength implied between model Canterbury and Otago (Figure 4) is much more significant than the difference in

actual values for either region if we were to alter the rheology to a granite-based upper crust and amphibolite-based lower crust rather than a quartzite/diabase crust for example.

4. Results

4.1. Model Surface Velocities

[25] The strength contrast in the model lower crust is reflected in the strain pattern at the surface as illustrated in the two components of displacement, parallel to and normal to the plate boundary (Figures 5a and 5b). In model Canterbury, plate-parallel motion is accommodated adjacent to the model plate boundary, while plate-normal displacement extends out to about 100 km east of the model boundary (Figures 5a and 5b). The net result is high strain rates in model Canterbury within ~60 km of the model Alpine Fault with the highest strain rates adjacent to the fault. In model Otago, both plate-parallel and plate-normal motion are taken up in a broad zone extending across much of the model region (Figures 5a and 5b). Some partitioning of deformation occurs with the plate-parallel motion gradually fanning out from the model Otago/Canterbury transition zone versus the sudden expansion of plate-normal motion across all of Otago at the transition.

[26] Model vertical uplift rates also reflects the along-strike rheological variation (Figure 5c). In model Canterbury, uplift is concentrated into a ~70 km wide band adjacent to the model Alpine Fault, with greatest uplift rates adjacent to the fault. Vertical motion in model Otago is more widespread with a region of moderate uplift rates adjacent to the model Alpine Fault with distributed low uplift rates extending eastward to the edge of the continent. A robust feature of this model is a region of high uplift rates where the transition from weak to strong lower crustal rheology intersects the model plate boundary.

4.2. Examination of Transition Between Displacement States Using Perturbation Theory

[27] The similarity of natural and model kinematics at a regional scale encourages some confidence in our chosen mechanical model. However, the surface displacement field
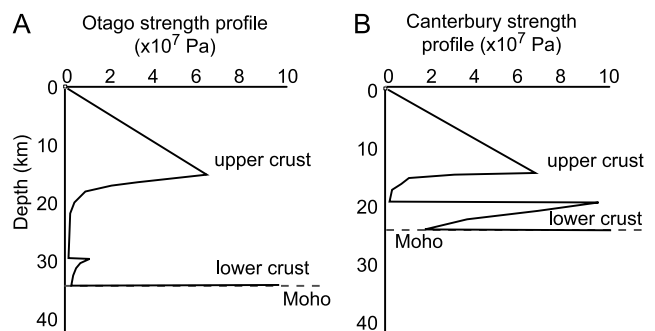

Figure 4. Crustal strength profiles for Otago and Canterbury used in the models. Based on a quartzite/diabase upper/lower crust. See text for more details.
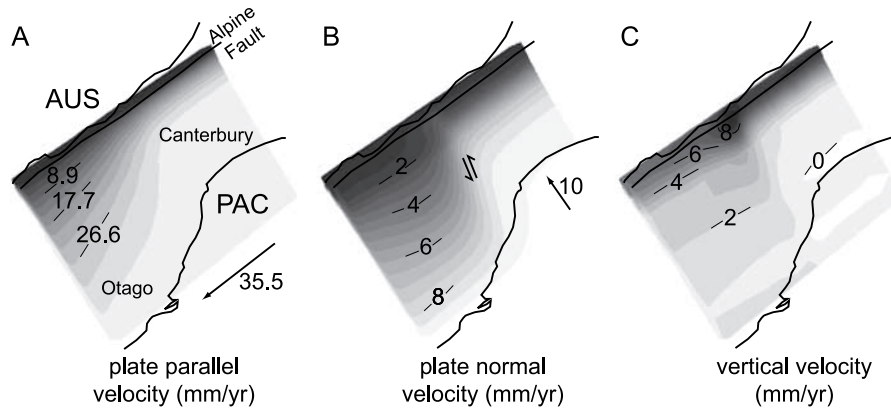
Figure 5. Model results overlain onto an outline of the South Island. (a) Contours of plate-parallel velocity relative to a fixed Pacific plate. (b) Contours of plate-normal velocity relative to a fixed Pacific plate. (c) Absolute uplift rate. See text for explanation.

that accommodates the regional kinematics contains more information on earth dynamics than is visible at the regional scale. The coexistence of at least two distinct displacement states, thrusting normal to, and thrusting parallel to, the plate boundary as discussed above (Figure 1a), suggests coexisting stress states with a stress transition analogous to that associated with displacement partitioning between strike slip and oblique thrusting regimes [*Enlow and Koons*, 1998]. Numerous phenomena that alter any of the coordinate stress components can cause minor changes of displacement orientation and provide limited constraint on stress states, however,

as discussed below the coexistence of distinct displacement states can only occur for a limited set of stress conditions and therefore severely restricts the degrees of freedom of the relative values of the coordinate stress tensor.

[28] Using perturbation theory for 3-D deforming Mohr-Coulomb wedges, *Enlow and Koons* [1998] demonstrated the conditions under which very different displacement states can be separated by minor stress differences. This transition between displacement states occurs with rapid rotation of the principal stress axes as they change their association with the coordinate stresses (Figure 6). The requisite conditions for
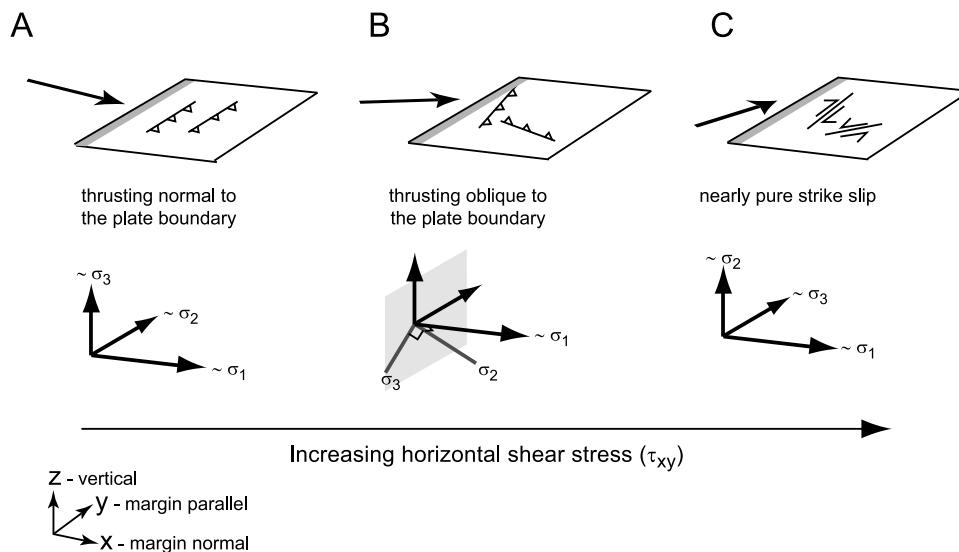

Figure 6. Relationship of coordinate stresses and principal stresses for a model orogen with increasing obliquity (Figures 6a to 6c) [*Koons*, 1994; *Enlow and Koons*, 1998]. As the relative motion becomes more oblique, the horizontal shear stress increases and the orientation of the principal stresses changes. (a) Initially, σ_1 is associated with margin-normal direction (x), σ_2 is associated with margin-parallel direction (y), and σ_3 is associated with the vertical (z). (b) As the horizontal shear stress increases, σ_2 and σ_3 rotate about the margin-parallel direction (x), staying close to the yz plane shown in light gray. (c) Eventually swapping such that σ_2 becomes associated with the vertical (z) and σ_3 becomes associated with the margin-parallel direction (y). The style of faulting changes from thrusting normal to the plate boundary (Figure 6a) through oblique thrusting (Figure 6b) to nearly pure strike slip (Figure 6c).

transition from predominantly reverse faulting to dominantly strike-slip faulting were shown to occur when

$$\tau_{xy} \rightarrow \hat{\tau} \equiv \sqrt{\tau_{xz}^2 + (\sigma_{xx} - \sigma_{yy})(\sigma_{yy} - \sigma_{zz})} \qquad (4)$$

τ_{xy} horizontal shear stress;
$\hat{\tau}$ characteristic stress [*Enlow and Koons*, 1998];
τ_{xz} shear stress in the $x - z$ plane;
σ_{xx} normal stress in the x direction;
σ_{yy} normal stress in the y direction;
σ_{zz} normal stress in the z direction.

[29] A dimensionless stress perturbation parameter, $\varepsilon^{\sigma_2 y \rightarrow z} \equiv \tau_{xy}/\hat{\tau}$ [*Enlow and Koons*, 1998] is used to represent how close a system is to transition. The symbol ε reflects the origin of the parameter from perturbation theory. The notation of this parameter refers to σ_2 (the intermediate principal stress) changing from being associated with the y coordinate axis to being associated with the z (vertical) coordinate axis.

[30] With increasing horizontal shear stress (τ_{xy}), the intermediate principal stress, σ_2, switches from being associated with the plate-parallel direction (y) to being associated with the vertical axis (z). This switch is accompanied by the equivalent switch of σ_3 from near vertical to near horizontal. These two minor stress axes rotate about the horizontal σ_1.

[31] An algebraic symmetry exists between this previously examined transition from thrusting to strike-slip (Figure 6), and the transition between oblique reverse faulting in approximately orthogonal directions (Figure 7). This symmetry allows transition to be expressed by an analogous dimensionless parameter, $\varepsilon^{\sigma_1 x \rightarrow y} \equiv \tau_{yz}/\hat{\tau}$. The notation of this parameter refers to σ_1 (the maximum principal stress) changing from being associated with the x coordinate axis to being associated with the y coordinate axis. This transition indicates a switching of the major principal axes between the two horizontal coordinates as they rotate about a near vertical axis; i.e., σ_1 switches from predominantly associated with the boundary-normal stress (σ_{xx}) to being predominantly associated with the boundary-parallel coordinate-normal stress (σ_{yy}) (Figure 7). Transition from boundary-normal thrusting to boundary-parallel thrusting occurs when $\varepsilon^{\sigma_1 x \rightarrow y}$ approaches unity either through an increase in τ_{yz} or by a reduction in $\hat{\tau}$ as

$$\tau_{yz} \rightarrow \hat{\tau} \equiv \sqrt{\tau_{xz}^2 + (\sigma_{xx} - \sigma_{yy})(\sigma_{yy} - \sigma_{zz})} \qquad (5)$$

τ_{yz} vertical shear stress in the yz plane;
$\hat{\tau}$ characteristic stress [*Enlow and Koons*, 1998];
τ_{xz} shear stress in the xz plane;
σ_{xx} normal stress in the x direction;
σ_{yy} normal stress in the y direction;
σ_{zz} normal stress in the z direction.

[32] The dimensionless parameter $\varepsilon^{\sigma_1 x \rightarrow y} < 1$ corresponds to σ_1 being associated with x and $\varepsilon^{\sigma_1 x \rightarrow y} > 1$ corresponds to σ_1 being associated with y; x is the convergence direction and thus σ_1 is most often associated with x, implying that $\varepsilon^{\sigma_1 x \rightarrow y}$ is most commonly <1.

[33] We extracted stress components from our three-dimensional mechanical model described above (Figure 5) and used them to calculate the spatial distribution of $\varepsilon^{\sigma_1 x \rightarrow y}$. We were then able to identify those regions where transition among displacement states is likely to occur (Figure 7a). The stress diagrams, calculated along a horizontal slice $\sim$8 km below the surface, show that generally $\varepsilon^{\sigma_1 x \rightarrow y} < 1$ over both the high and low strength regions where we predict that only boundary-normal thrusting is likely to occur (Figure 7a). However, $\varepsilon^{\sigma_1 x \rightarrow y} \geq 1$ over the boundary between high strength and low strength regions (model Canterbury−model Otago) due to a local increase in both τ_{yz} and the ratio of the coordinate-normal stresses, $\gamma^{\sigma_1 x \rightarrow y} = \sigma_{yy}/\sigma_{xx}$ (Figures 7b and 7c). Consequently, transition from boundary-normal to boundary-parallel oblique thrusting is predicted over the model rheological boundary.

[34] In oblique convergence using the convention shown in Figure 3, σ_{xx} is associated with the normal to the plate boundary and, as indicated by the ratio of the two horizontal compressive stresses, σ_{yy}/σ_{xx} (γ^{xy}) in the strong-based Canterbury region, is the dominant normal stress (Figure 7b). The magnitude of σ_2 in a Mohr-Coulomb material is constrained only to lie between that of the other principal stresses and differs from the coordinate stress σ_{yy} as a function of the shear stresses, τ_{xy} and τ_{yz}. An increase in the horizontal shear stress, τ_{xy}, reduces σ_2, while increased shear stress in the vertical plane, τ_{yz}, increases σ_2. When the magnitude of σ_{yy} approaches that of σ_{xx}, then either an increase in τ_{yz} or a reduction in τ_{xz} can cause the magnitude of σ_2 to reach that of σ_1. Under these conditions, the coexistence of reverse faulting on orthogonal displacement planes is possible for minor shifts in shear stresses [*Enlow and Koons*, 1998].

[35] In summary, the coexistence of orthogonal reverse fault systems is favored by σ_{yy} approaching σ_{xx} and increasing vertical shear stress parallel to the plate boundary, τ_{yz} so that $\varepsilon^{\sigma_1 x \rightarrow y}$ approaches 1 (Figure 7). The vertical rheological boundary created by the change in crustal thickness and strength imposes an additional vertical shear stress in this region, which is transmitted up through the brittle crust. In the central South Island, coexistence of orthogonal thrusting directions associated with the schist to graywacke transition are compatible with a rheological transition from weak to strong lower crust.

[36] Models were also run in which the width of the transition zone was varied (see Figure S1 in the auxiliary material).[1] As the width of the transition zone was increased to up to 100 km, the model results were largely unchanged. The zone of $\varepsilon^{\sigma_1 x \rightarrow y} > 1$ becomes narrower and is shifted slightly toward to stronger crust (see Figure S1).

5. Discussion

[37] Oblique convergence of the model crust with differing lower crustal strengths results in an increased width of deformation and lower strain rates over the weak zone relative to the strong region (Figure 5). This is to be expected because

---

[1] Auxiliary materials are available in the HTML. doi:10.1029/ 2008TC002353.
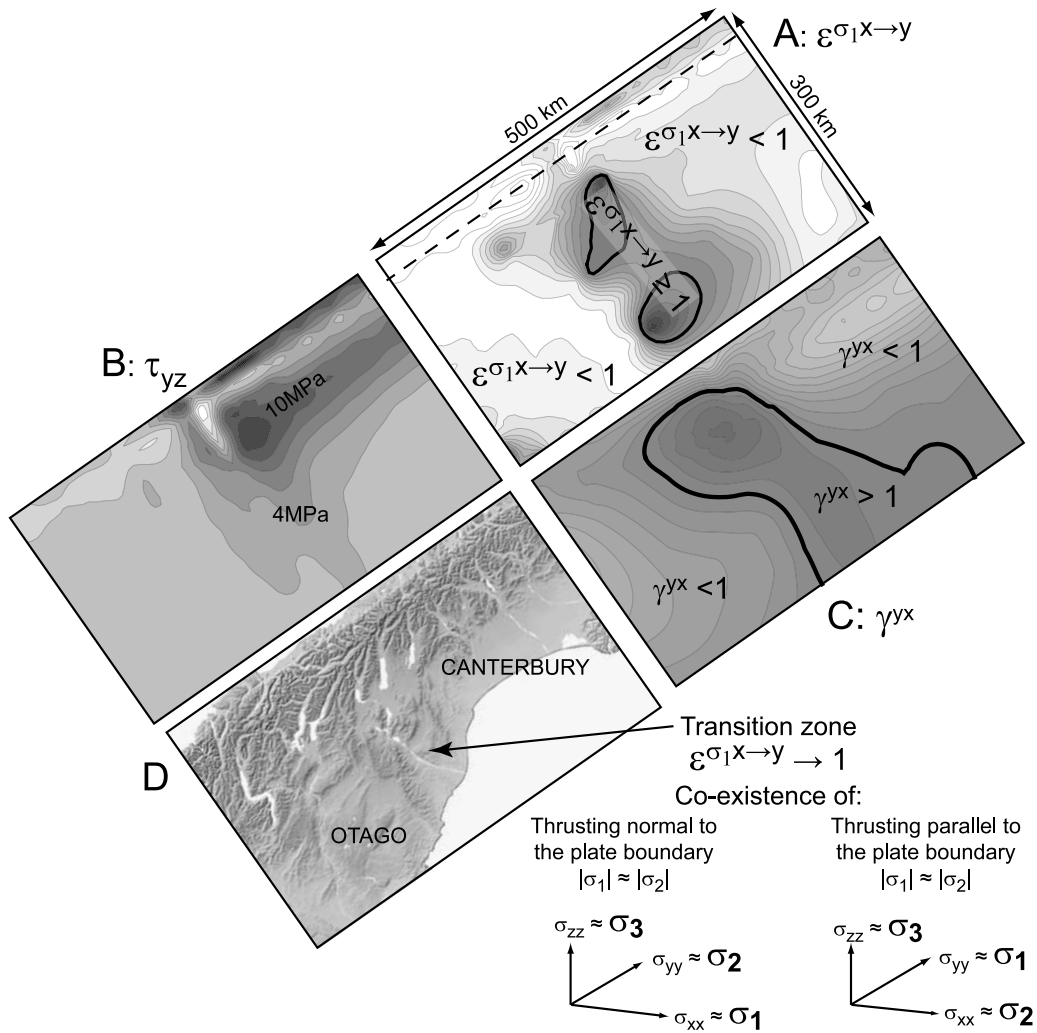
Figure 7. Analysis of the model stress tensor to look for coexisting stress states [*Enlow and Koons*, 1998]. Sections are from 8 km depth within the model. (a) The parameter $\varepsilon^{\sigma_1 x \to y}$ (see text for definition). Contours range from 0 (white) to 2 (black). Dashed line represents model Alpine Fault; $\varepsilon^{\sigma_1 x \to y}$ is generally <1 except over the transition region from model Canterbury to model Otago. (b) The parameter τ_{yz}, horizontal shear stress across the model region; τ_{yz} increases across the transition from model Canterbury to model Otago. Contours range from 0 (white) to 12 MPa (dark gray). (c) The parameter γ^{yx}, the ratio of coordinate-normal stresses. Contours range from 0 (white) to 2 (black). (d) DEM of the transition between Canterbury and Otago. The transition zone is a region where $\varepsilon^{\sigma_1 x \to y}$ approaches 1 with coexistence of thrusting normal to and thrusting parallel to the plate boundary.

the weak lower crust is unable to sustain high stresses and will consequently fail over a larger region while failure in the strong lower crust will be more confined adjacent to the plate boundary. However, the surface displacement field of the South Island contains more information than is visible at the regional scale. By using our three-dimensional mechanical models and examining the resulting stress states using perturbation theory we are able to extract stress components and to investigate the implications of this rheological variation for other processes such as surface faulting, timing and localization of uplift, fluid flow and gold mineralization.

5.1. Geological Consequences

[38] The different crustal thicknesses and rheologies of Canterbury and Otago, that are a consequence of their mode of formation, have governed many features of their subsequent geological history. Comparison of geology and our modeling results allows us to offer an explanation for some of the features of the Southern Alps that vary along strike from Canterbury in the north and Otago in the south.

5.1.1. Partitioning and Width of Deformation

[39] The model results compare favorably with observations from the South Island, where deformation and uplift

extend to the coast in Otago but are restricted to about 70 km east of the Alpine Fault in Canterbury. Partitioning of the horizontal velocity components is more pronounced where the lower crust is weak as predicted from analytical analysis [*Enlow and Koons*, 1998] and observed in model results [*Upton et al.*, 2003b]. *Norris and Cooper* [2001] show that there is clear evidence in the slip rate data for increasing partitioning toward the south of the fault-normal component onto structures other than the Alpine Fault, while the amount of fault-parallel displacement taken up on the Alpine Fault remains relatively constant along the length of the boundary. In the early states of model convergence while deformation in both Canterbury and Otago is expanding most rapidly, a zone of sinistral displacement develops between the weak and strong base blocks at high angle to the plate boundary (Figure 5b). Recent movement along the Wharekuri Fault, within the transition between Canterbury and Otago and approximately normal to the plate boundary, as well as geodetic analysis shows similar sinistral kinematics over the long term [*Gair and Gregg*, 1960; *Forsyth*, 2002] and anticlockwise rotation in the modern geodetic field [*Pearson*, 1990; *Henderson*, 2003].

5.1.2. Localization of Normal Faults

[40] The exact geometry of the transition between thick and thin crust, constructed in the Mesozoic, is unknown because of subsequent modification. The thickness transition became the locus for normal faulting in the middle Cretaceous, and this has accentuated the Canterbury-Otago boundary. The most prominent feature of this boundary at the surface is the Waihemo-Hawkdun Fault system and related structures (Figure 1a). This fault system juxtaposes prehnite-pumpellyite facies metagraywackes of Canterbury against greenschist facies schists of Otago via a series of narrow northwest striking fault slices over a 5–10 km wide zone [*Forsyth*, 2002; *MacKenzie and Craw*, 2006]. Gently dipping normal faults subparallel to schist foliation immediately SW of the Waihemo-Hawkdun Fault system were related to this mid-Cretaceous extension, and these also juxtaposed rocks of differing metamorphic grade in the transition between schist and graywacke [*Deckert et al.*, 2003; *Craw et al.*, 2007].

5.1.3. Localization of Initial Alpine Fault Uplift

[41] The Alpine Fault was initiated in the late Oligocene–early Miocene as the new plate boundary formed through the New Zealand crustal block [*Cooper et al.*, 1987]. Transpression associated with this new plate boundary occurred initially in the thick weak crust of NW Otago, with development of a 30 km wide deformation zone between the Alpine Fault and the Moonlight Fault (Figure 1a) [*Cooper et al.*, 1987; *Craw*, 1995]. Uplift associated with this deformation resulted in initiation of the Southern Alps in that area and the mountain range subsequently developed northeast from there [*Craw*, 1995].

5.1.4. Localization of Maximum Uplift

[42] Measured rock uplift rates, thermochronology, and geological and geodetic observations suggest that the central section of the Southern Alps, including Mount Cook-Aoraki and the Fox and Franz Josef glaciers, appears to be undergoing more rapid rock uplift than surrounding parts of the orogen [*Simpson et al.*, 1994; *Norris and Cooper*, 2001; *Little*

et al., 2005]. This region is near the intersection of the Canterbury-Otago boundary with the Alpine Fault zone. Models put forward to explain this observation include the existence of a restraining bend in the Alpine Fault at depth in this region [*Little et al.*, 2005]. In our model we see a region of higher uplift at this boundary. Uplift is enhanced as the stronger lower crust of model Canterbury acts as an indentor into the weaker lower crust of model Otago. Model Otago material is extruded upward as a result of this indentation, leading to a region of higher rock uplift rate centered on the model Otago side of the transition [*Upton and Koons*, 2007]. The resolution of our numerical models is such that, while we can predict the deformation style at various regions within the orogen, we cannot predict the specific nature of the geological structures that might accommodate this deformation in nature. These structures will develop as a result of the factors discussed in this manuscript as well as local variability in rock properties and surfacial boundary conditions. A region of possible interconnected pore fluids in the midcrust, as imaged by magnetotellurics [*Wannamaker et al.*, 2002] may also contribute to the development of this region of higher uplift [*Upton and Koons*, 2007].

5.1.5. Current Motion on the Canterbury-Otago Boundary

[43] The middle Cretaceous normal faults at the Canterbury-Otago boundary have been reactivated during the late Tertiary plate boundary deformation, and many of these faults are currently active. The Waihemo-Hawkdun and Waitaki fault systems (Figure 1a) have several active strands [*Forsyth*, 2002]. Most of this active deformation is dominated by the vertical component, and the Waihemo-Hawkdun Fault system has had nearly 2 km of uplift on the Canterbury side (Figure 1a). In addition, there is also evidence for active sinistral motion on faults at the Canterbury-Otago boundary, which is unusual in New Zealand's dominantly dextral tectonic setting. The sinistral motion is most evident on the Waitaki Fault system, on the Wharekuri Fault [*Forsyth*, 2002], and also on a strand of the Ostler Fault system immediately NW along the Canterbury-Otago boundary [*Templeton et al.*, 1999] (Figure 2a).

5.1.6. Displacement Partitioning at the Transition

[44] Along the transition zone between Canterbury and Otago, both NE and NW striking thrusts are active, implying that σ_1 and σ_2 are of similar magnitude and easily switched [*Enlow and Koons*, 1998]. This switching is facilitated by an increase in τ_{yz} and/or an increase in the ratio σ_{yy}/σ_{xx} (Figures 7b and 7c). Both occur over the transition from a strong to weak lower crust, such as occurs between Canterbury and Otago.

[45] A similar situation exists on the northern Colorado Plateau where kinematic analysis of Laramide basement-cored uplifts indicate that at least four major uplifts were formed by northeast directed shortening while at least two more were constructed by southeast directed shortening [*Kelley and Clinton*, 1960; *Jamison and Stearns*, 1982; *Anderson and Barnhard*, 1986; *Davis*, 1999; *Tindall and Davis*, 1999; *Bump and Davis*, 2003]. Available timing data for these uplifts are scant but point to simultaneous rise of both sets of uplifts [*Lawton*, 1983; *Goldstrand*, 1994; *Bump*, 2004]. *Bump* [2004]

proposes that the different shortening directions are a predictable result of deformation in a three-dimensional stress field where the magnitude of σ_2 approaches that of σ_1. Tectonically, σ_1 may have resulted from coupling between the horizontally subducting Farallon slab and the North American plate [*Bump*, 2004]. The elevated values of σ_2 were attributed to far-field stresses generated by the topographically high Sevier thrust belt which was active at the time of deformation in the plateau [*Bump*, 2004].

5.2. Gold Mineralization

[46] Hydrothermal gold mineralization accompanied several stages of the Miocene-Recent tectonic activity described above. Gold-bearing fluids were generated by metamorphic dehydration reactions, particularly associated with greenschist facies metamorphism [*Craw et al.*, 2002; *Pitcairn et al.*, 2006]. These fluids were channeled to sites of gold deposition via structures formed during synchronous deformation [*Craw et al.*, 2002]. Hence, formation of gold deposits was intimately linked to the tectonic evolution of the crust, and there are some clear controls on distribution of gold deposits related to the differences in crustal thicknesses and rheologies between Canterbury and Otago.

5.2.1. Miocene Gold

[47] Deformation and uplift of thick Otago crust during initiation of the Alpine Fault and Southern Alps (above) were accompanied by gold mineralization [*Craw et al.*, 2007]. Emplacement of gold-bearing veins was intimately related to deformation along the Moonlight Fault (Figure 1a). The veins occur in Aspiring Terrane schists that underlie the Torlesse Terrane in the thick Otago schist pile of NW Otago [*Norris and Craw*, 1987]. The Aspiring Terrane contains abundant chlorite-rich metabasites that may have generated fluids at depth during the Miocene deformation [*Norris and Craw*, 1987; *Craw et al.*, 2007]. In contrast, there is no evidence for this style of deformation or gold mineralization in Canterbury during the Miocene. The thinner Canterbury crust, lack of fertile Aspiring Terrane source, and lack of focused Miocene deformation are the probable reasons for the lack of Canterbury Miocene gold, and these are all related to the differences in crustal structure and rheology between Canterbury and Otago.

5.2.2. Plio-Pleistocene Gold

[48] A belt of small gold deposits occurs near the crest of the Canterbury portion of the Southern Alps, and these formed during Plio-Pleistocene uplift and deformation adjacent to the Alpine Fault [*Craw et al.*, 2002]. Mineralizing fluids have been, and are being, generated in the middle crustal portion of the narrow thickened root beneath the Southern Alps, and these fluids rise buoyantly along fractures beneath the main mountain chain [*Craw et al.*, 2002; *Upton and Koons*, 2007]. These processes operating in the Southern Alps of Canterbury are similar to those that operated at the Miocene inception of the Southern Alps in Otago (section 5.2.1), but the resultant veins are temporally and spatially distinct. Gold mineralization ceased in Otago when the orogen changed from a narrow focused zone in the Miocene to the present wide orogen, and the gold mineral-

ization system stepped up to the narrow focused Canterbury portion of the orogen.

6. Conclusions

[49] As with most natural materials, the Earth's crust exhibits a path-dependent rheology, with a memory dependent upon deformation (including strain and thermal evolution) history [e.g., *Koons et al.*, 2003; *Jamieson et al.*, 2004]. The Southern Alps of New Zealand are a highly three-dimensional mountain belt that cannot be adequately modeled using a two-dimensional description in which properties vary only normal to the plate boundary. We suggest that many features of the long-term displacement field of this region can be produced using a simple along-strike variation in the rheological model of the crust subjected to far-field driving velocities derived from plate tectonic observations. At the orogen scale, the increasing width of the orogen is compatible with reduced flow resistance at depth beneath the southern Otago portion of the plate boundary where geological studies suggest a deeper, weaker continental crust. At suborogen scale, the coexistence of contrasting displacement states in the transition region of eastern New Zealand is also compatible with the same rheological model. The perturbation-derived variable used here, $\varepsilon^{\sigma_1 x \rightarrow y} \equiv \tau_{yz}/\hat{\tau}$, provides a means of evaluating crustal stress states where displacement partitioning is observed.

[50] The different modes of formation, crustal thicknesses and rheologies of the Canterbury and Otago regions govern many features of their subsequent geological histories. The boundary becomes the locus for normal faulting in the middle Cretaceous, which accentuated the Canterbury/Otago boundary. Alpine Fault related uplift initially occurred in the thick weak crust of NW Otago and subsequently migrated to the northwest from there. At the present day, the central Southern Alps are uplifting more rapidly than regions to the north and south. The locus of rapid and maximum uplift is spatially coincident with the intersection of the Canterbury/Otago boundary with the Alpine Fault. Our models suggest that this results from the stronger lower crust of Canterbury indenting the weaker Otago crust, causing Otago crust to be extruded upward.

[51] Hydrothermal gold mineralization in the Torlesse terrane was intimately linked to the tectonic evolution of the crust and there are clear controls on gold distribution resulting from the Canterbury/Otago differences. Focused deformation in Otago in the Miocene was accompanied by gold mineralization. Canterbury was barren of gold deposits until the Plio-Pleistocene when mineralizing fluids were generated in the middle crustal portion of the narrow thickening root being the Southern Alps. At present gold is not being produced beneath Otago, either because prograde metamorphism is too slow to produce the required fluid or the low strain rates do not produce the deformation-induced permeability and fluid flow required for its production.

[52] Our successful application of experimentally derived crustal strength profiles within our continuum model framework of the central South Island by no means provides proof

of our rheological model. Other combinations of rheology and varying boundary conditions may be capable of producing similar results. However, similarity of field observations and numerical results from our simple model based upon temperature-dependent crustal rheology indicates that the "jelly sandwich" rheological model is a permissible model in this instance. This model is sufficient to reproduce strain observations at both the lithospheric scale of the South Island orogen and at the scale of the local structures where displacement partitioning occurs.

References

Amos, C. B., D. W. Burbank, D. C. Nobes, and S. A. L. Read (2007), Geomorphic constraints on listric thrust faulting: Implications for active deformation in the Mackenzie Basin, South Island, New Zealand, *J. Geophys. Res.*, *112*, B03S11, doi:10.1029/2006JB004291.

Anderson, R. E., and T. P. Barnhard (1986), Genetic relationship between faults and folds and determination of Laramide and neotectonic paleostress, western Colorado Plateau transition zone, *Tectonics*, *5*, 335–357, doi:10.1029/TC005i002p00335.

Baldock, G., and T. Stern (2005), Width of mantle deformation across a continental transform: Evidence from upper mantle (Pn) seismic anisotropy measurements, *Geology*, *33*, 741–744, doi:10.1130/G21605.1.

Barnes, P., R. Sutherland, and J. Delteil (2005), Strike-slip structure and sedimentary basins of the southern Alpine Fault, Fiordland, New Zealand, *Geol. Soc. Am. Bull.*, *117*, 411–435, doi:10.1130/B25458.1.

Beaumont, C., P. Fullsack, and J. Hamilton (1992), Erosional control of active compressional orogens, in *Thrust Tectonics*, edited by K. R. McClay, pp. 1–18, Chapman and Hall, New York.

Beavan, J., et al. (1999), Crustal deformation during 1994–1998 due to oblique continental collision in the central Southern Alps, New Zealand, and implications for seismic potential of the Alpine fault, *J. Geophys. Res.*, *104*, 25,233–25,255, doi:10.1029/1999JB900198.

Beavan, J., S. Ellis, L. Wallace, and P. Denys (2007), Kinematic constraints from GPS on oblique convergence of the Pacific and Australian plates, central South Island, New Zealand, in *A Continental Plate Boundary: Tectonics at South Island, New Zealand*, *Geophys. Monogr. Ser.*, vol. 175, edited by D. Okaya, T. Stern, and F. Davey, pp. 75–94, AGU, Washington, D. C.

Blick, G. H., S. A. L. Read, and P. T. Hall (1989), Ostler Fault zone: Progress report on surveying results 1966–1985, levelling and tilt leveling, *Rep. EDS 102*, N. Z. Geol. Surv., Lower Hutt.

Bourguignon, S., T. A. Stern, and M. K. Savage (2007), Crust and mantle thickening beneath the southern portion of the Southern Alps, New Zealand, *Geophys. J. Int.*, *168*, 681–690, doi:10.1111/j.1365-246X.2006.03208.x.

Bradshaw, J. D. (1989), Cretaceous geotectonic patterns in the New Zealand region, *Tectonics*, *8*, 803–820, doi:10.1029/TC008i004p00803.

Bump, A. P. (2004), Three-dimensional Laramide deformation of the Colorado Plateau: Competing stresses from the Sevier thrust belt and the flat Farallon slab, *Tectonics*, *23*, TC1008, doi:10.1029/2002TC001424.

Bump, A. P., and G. H. Davis (2003), Late Cretaceous–early Tertiary deformation of the northern Colorado Plateau, Colorado and Utah, *J. Struct. Geol.*, *25*, 421–440, doi:10.1016/S0191-8141(02)00033-0.

Burov, E. B., and A. B. Watts (2006), The long-term strength of continental lithosphere: "jelly sandwich" or "crème brûlèe"?, *GSA Today*, *16*, 4–10,

doi:10.1130/1052-5173(2006)016<4:TLTSOC>2.0.CO;2.

Chen, W.-P., and P. Molnar (1983), Focal depths of intracontinental and intraplate earthquakes and their implications for the thermal and mechanical properties of the lithosphere, *J. Geophys. Res.*, *88*, 4183–4214, doi:10.1029/JB088iB05p04183.

Coombs, D. S., C. A. Landis, R. J. Norris, J. M. Sinton, D. J. Borns, and D. Craw (1976), The Dun Mountain ophiolite belt, New Zealand, its tectonic setting, construction, and origin, with special reference to the southern portion, *Am. J. Sci.*, *276*, 561–603.

Cooper, A. F., B. A. Barreiro, D. L. Kimbrough, and J. M. Mattinson (1987), Lamprophyre dike intrusion and the age of the Alpine Fault, New Zealand, *Geology*, *15*, 941–944, doi:10.1130/0091-7613(1987)15<941:LDIATA>2.0.CO;2.

Cox, S. C., and R. H. Findlay (1995), The Main Divide Fault Zone and its role in formation of the Southern Alps, New Zealand, *N. Z. J. Geol. Geophys.*, *38*, 489–499.

Cox, S. C., and R. S. Sutherland (2007), Regional geological framework of South Island, New Zealand, and its significance for understanding the active plate boundary, in *A Continental Plate Boundary: Tectonics at South Island, New Zealand*, *Geophys. Monogr. Ser.*, vol. 175, edited by D. Okaya, T. Stern, and F. Davey, pp. 19–46, AGU, Washington, D. C.

Craw, D. (1995), Reinterpretation of the erosion profile across the southern portion of the Southern Alps, Mt Aspiring area, Otago, New Zealand, *N. Z. J. Geol. Geophys.*, *38*, 501–507.

Craw, D. (1998), Structural boundaries and biotite and garnet 'isograds' in the Otago and Alpine Schists, New Zealand, *J. Metamorph. Geol.*, *16*, 395–402, doi:10.1111/j.1525-1314.1998.00143.x.

Craw, D., P. O. Koons, T. Horton, and C. P. Chamberlain (2002), Tectonically driven fluid flow and gold mineralisation in active collisional orogenic belts: Comparison between New Zealand and western Himalaya, *Tectonophysics*, *348*, 135–153, doi:10.1016/S0040-1951(01)00253-0.

Craw, D., D. J. MacKenzie, I. K. Pitcairn, D. A. H. Teagle, and R. J. Norris (2007), Geochemical signatures of mesothermal Au-mineralised late-metamorphic deformation zones, Otago Schist, NZ, *Geochem. Explor. Environ. Anal.*, *7*, 225–232, doi:10.1144/1467-7873/07-137.

Cundall, P., and M. Board (1988), A microcomputer program for modelling of large-strain plasticity problems, in *Numerical Methods in Geomechanics: Proceedings of the 6th International Conference on Numerical Methods in Geomechanics, Innsbruck, 11–15 April 1988*, edited by C. Swoboda, pp. 101–108, A. A. Balkema, Rotterdam, Netherlands.

Davis, G. H. (1999), Structural Geology of the Colorado Plateau Region of Southern Utah With Special Emphasis on Deformation Bands, *Spec. Pap. Geol. Soc. Am.*, *342*, 157 pp.

Deckert, H., U. Ring, and N. Mortimer (2003), Tectonic significance of Cretaceous bivergent extensional

shear zones in the Torlesse accretionary wedge, central Otago Schist, New Zealand, *N. Z. J. Geol. Geophys.*, *45*, 537–547.

DeMets, C., R. G. Gordon, D. F. Argus, and S. Stein (1994), Effect of recent revisions to the geomagnetic reversal time scale on estimates of current plate motions, *Geophys. Res. Lett.*, *21*, 2191–2194, doi:10.1029/94GL02118.

Eberhart-Phillips, D., and S. Bannister (2002), Three-dimensional crustal structure in the Southern Alps region of New Zealand from inversion of local earthquake and active source data, *J. Geophys. Res.*, *107*(B10), 2262, doi:10.1029/2001JB000567.

Eberhart-Phillips, D., and M. Reyners (1997), Continental subduction and three-dimensional crustal structure: The northern South Island, New Zealand, *J. Geophys. Res.*, *102*, 11,843–11,861, doi:10.1029/96JB03555.

Eberhart-Phillips, D., and M. Reyners (2001), A complex, young subduction zone imaged by three-dimensional seismic velocity, Fiordland, New Zealand, *Geophys. J. Int.*, *146*, 731–746, doi:10.1046/j.0956-540x.2001.01485.x.

Ellis, S., J. Beavan, and D. Eberhart-Phillips (2006), Bounds on the width of mantle lithosphere flow derived from surface geodetic measurements: Application to the central Southern Alps, New Zealand, *Geophys. J. Int.*, *166*, 403–417, doi:10.1111/j.1365-246X.2006.02918.x.

Enlow, R. L., and P. O. Koons (1998), Critical wedges in three dimensions: Analytical expressions from Mohr-Coulomb constrained perturbation analysis, *J. Geophys. Res.*, *103*, 4897–4914, doi:10.1029/97JB03209.

Forsyth, P. J. (2002), Geology of the Waitaki area, *Geol. Map 19*, scale, 1:250,000 1 sheet + 64 pp., N. Z. Inst. of Geol. and Nucl. Sci. Ltd., Lower Hutt.

Gair, H. S., and D. R. Gregg (1960), Relation of Kakanui Schist to Kaihikuan sedimentary rocks at Mt St Mary, North Otago, *N. Z. J. Geol. Geophys.*, *3*, 618–625.

Gerbault, M., S. Henrys, and F. Davey (2003), Numerical models of lithospheric deformation forming the Southern Alps of New Zealand, *J. Geophys. Res.*, *108*(B7), 2341, doi:10.1029/2001JB001716.

Ghisetti, F. C., A. R. Gorman, and R. H. Sibson (2007), Surface break-through of a basement fault by repeated episodes of seismic slip: The Ostler Fault, South Island, New Zealand, *Tectonics*, *26*, TC6004, doi:10.1029/2007TC002146.

Goldstrand, P. M. (1994), Tectonic development of Upper Cretaceous to Eocene strata of southwestern Utah, *Geol. Soc. Am. Bull.*, *106*, 145–154, doi:10.1130/0016-7606(1994)106<0145:TDOUCT>2.3.CO;2.

Gray, D. R., and D. A. Foster (2004), $^{40}Ar/^{39}Ar$ thermochronologic constraints on deformation, metamorphism and cooling/exhumation of a Mesozoic accretionary wedge, Otago Schist, New Zealand, *Tectonophysics*, *385*, 181–210, doi:10.1016/j.tecto.2004.05.001.

Henderson, C. M. (2003), The velocity field of the South Island of New Zealand derived from GPS

and terrestrial measurements, Ph.D. thesis, Univ. of Otago, Dunedin, New Zealand.

Jackson, J. A., R. J. Norris, and J. H. Youngson (1996), The structural evolution of active fault and fold systems in Central Otago, New Zealand: Evidence revealed by drainage patterns, *J. Struct. Geol.*, *18*, 217–234, doi:10.1016/S0191-8141(96)80046-0.

James, Z. (1998), Geology, Quaternary structure, fault rocks and fluid flow, Fox Peak Range, eastern Southern Alps, M.Sc. thesis, Univ. of Otago, Dunedin, New Zealand.

Jamieson, R. A., C. Beaumont, S. Medvedev, and M. H. Nguyen (2004), Crustal channel flows: 2. Numerical models with implications for metamorphism in the Himalayan-Tibetan Orogen, *J. Geophys. Res.*, *109*, B06407, doi:10.1029/2003JB002811.

Jamison, W. R., and D. W. Stearns (1982), Tectonic deformation of Wingate Sandstone, Colorado National Monument, *AAPG Bull.*, *66*, 2584–2608.

Kelley, V. C., and N. J. Clinton (1960), Fracture systems and tectonic elements of the Colorado Plateau, *Publ. Geol. 6*, Univ. of N. M., Albuquerque.

Kohler, M. D., and D. Eberhart-Phillips (2003), Intermediate-depth earthquakes in a region of continental convergence: South Island, New Zealand, *Bull. Seismol. Soc. Am.*, *93*, 85–93, doi:10.1785/0120020043.

Koons, P. O. (1990), Two-sided orogen: Collision and erosion from the sandbox to the Southern Alps, New Zealand, *Geology*, *18*, 679–682, doi:10.1130/0091-7613(1990)018<0679:TSOCAE>2.3.CO;2.

Koons, P. O. (1994), Three-dimensional critical wedges: Tectonics and topography in oblique collisional orogens, *J. Geophys. Res.*, *99*, 12,301–12,315, doi:10.1029/94JB00611.

Koons, P. O., D. Craw, S. C. Cox, P. Upton, A. S. Templeton, and C. P. Chamberlain (1998), Fluid flow during active oblique convergence: A Southern Alps model from mechanical and geochemical observations, *Geology*, *26*, 159–162, doi:10.1130/0091-7613(1998)026<0159:FFDAOC>2.3.CO;2.

Koons, P. O., R. J. Norris, D. Craw, and A. F. Cooper (2003), Influence of exhumation on the structural evolution of transpressional plate boundaries: An example from the Southern Alps, New Zealand, *Geology*, *31*, 3–6, doi:10.1130/0091-7613(2003)031<0003:IOEOTS>2.0.CO;2.

Laird, M. G. (1993), Cretaceous continental rifts; New Zealand region, in *Sedimentary Basins of the World*, vol. 2, *South Pacific Sedimentary Basins*, edited by P. F. Balance, pp. 37–49, Elsevier, Amsterdam.

Landis, C. A., H. J. Campbell, J. G. Begg, D. C. Mildenhall, A. M. Paterson, and S. A. Trewick (2008), The Waipounamu erosion surface: Questioning the antiquity of the New Zealand land surface and terrestrial fauna and flora, *Geol. Mag.*, *145*, 173–197, doi:10.1017/S0016756807004268.

Lawton, T. F. (1983), Late Cretaceous fluvial systems and the age of foreland uplifts in central Utah, in *Rocky Mountain Foreland Basins and Uplifts*, edited by J. D. Lowell and R. R. Gries, pp. 181–199, Rocky Mtn. Assoc. of Geol., Denver, Colo.

LeMasurier, W. E., and C. A. Landis (1996), Mantle-plume activity recorded by low-relief erosion surfaces in West Antarctica and New Zealand, *Geol. Soc. Am. Bull.*, *108*, 1450–1466, doi:10.1130/0016-7606(1996)108<1450:MPARBL>2.3.CO;2.

Little, T. A., and A. Jones (1998), Seven million years of strike-slip and off-fault deformation on the Awatere Fault, South Island, New Zealand, *Tectonics*, *17*, 285–302, doi:10.1029/97TC03148.

Little, T. A., S. Cox, J. K. Vry, and G. Batt (2005), Variations in exhumation level and uplift rate along the oblique-slip Alpine fault, central Southern Alps, New Zealand, *Geol. Soc. Am. Bull.*, *117*, 707–723, doi:10.1130/B25500.1.

Liu, Z., and P. Bird (2006), Two-dimensional and three-dimensional finite element modeling of mantle processes beneath central South Island, New Zealand, *Geophys. J. Int.*, *165*, 1003–1028, doi:10.1111/j.1365-246X.2006.02930.x.

MacKenzie, D. J., and D. Craw (2006), Paragenesis of hydrothermal minerals in the Rise and Shine Shear Zone, Otago Schist, paper presented at AusIMM Conference, Australasian Inst. of Min. and Metall., Waihi, N. Z.

MacKinnon, T. C. (1983), Origin of the Torlesse terrane and coeval rocks, South Island, New Zealand, *Geol. Soc. Am. Bull.*, *94*, 967–985, doi:10.1130/0016-7606(1983)94<967:OOTTTA>2.0.CO;2.

Markley, m., and R. J. Norris (1999), Structure and neotectonics of the Blackstone Hill Antiform, central Otago, New Zealand, *N. Z. J. Geol. Geophys.*, *42*, 205–218.

Melhuish, A., W. S. Holbrook, F. Davey, D. Okaya, and T. A. Stern (2005), Crustal and upper mantle seismic structure of the Australian plate, South Island, New Zealand, *Tectonophysics*, *395*, 113–135, doi:10.1016/j.tecto.2004.09.005.

Molnar, P., et al. (1999), Continuous deformation versus faulting through the continental lithosphere of New Zealand, *Science*, *286*, 516–519, doi:10.1126/science.286.5439.516.

Moore, M., P. England, and B. Parsons (2002), Relation between surface velocity field and shear wave splitting in the South Island of New Zealand, *J. Geophys. Res.*, *107*(B9), 2198, doi:10.1029/2000JB000905.

Mortimer, N. (1993a), Jurassic tectonic history of the Otago Schist, New Zealand, *Tectonics*, *12*, 237–244, doi:10.1029/92TC01563.

Mortimer, N. (1993b), Geology of the Otago Schist and adjacent rocks, *Geol. Map 7*, scale 1:500,000, N. Z. Inst. Geol. Nucl. Sci. Ltd., Lower Hutt.

Mortimer, N. (2000), Metamorphic discontinuities in orogenic belts: Example of garnet-biotite-albite zone in the Otago Schist, New Zealand, *Int. J. Earth Sci.*, *89*, 295–306, doi:10.1007/s005310000086.

Norris, R. J., and A. F. Cooper (2001), Late Quaternary slip rates and slip partitioning on the Alpine Fault, New Zealand, *J. Struct. Geol.*, *23*, 507–520, doi:10.1016/S0191-8141(00)00122-X.

Norris, R. J., and D. Craw (1987), Aspiring terrane: An oceanic assemblage from New Zealand and its implications for terrane accretion in the southwest Pacific, *Geodynamics*, *19*, 169–177.

Norris, R. J., P. O. Koons, and A. F. Cooper (1990), The oblique-convergent plate boundary in the South Island of New Zealand: Implications for ancient collision zones, *J. Struct. Geol.*, *12*, 715–725, doi:10.1016/0191-8141(90)90084-C.

Paterson, M. S., and F. C. Luan (1990), Quartzite rheology under geological conditions, in *Deformation Mechanisms, Rheology and Tectonics*, edited by R. J. Knipe and E. H. Rutter, *Geol. Soc. Spec. Publ.*, *54*, pp. 299–307.

Pearson, C. J. (1990), Extent and tectonic significance of the central Otago shear strain anomaly, *N. Z. J. Geol. Geophys.*, *33*, 295–301.

Pitcairn, I. K., D. H. Teagle, D. Craw, G. R. Olivo, R. Kerrich, and T. S. Brewer (2006), Sources of metals and fluids in orogenic gold deposits: Insights from the Otago and Alpine schists, New Zealand, *Econ. Geol.*, *101*, 1525–1546, doi:10.2113/gsecongeo.101.8.1525.

Savage, M. K., A. Tommasi, S. Ellis, and J. Chery (2007), Modeling strain and anisotropy along the Alpine Fault, South Island, New Zealand, in *A Continental Plate Boundary: Tectonics at South Island, New Zealand, Geophys. Monogr. Ser.*, vol. 175, edited by D. Okaya, T. Stern, and F. Davey, pp. 291–308, AGU, Washington, D. C.

Scherwath, M., T. Stern, F. Davey, D. Okaya, W. S. Holbrook, R. Davies, and S. Kleffmann (2003), Lithospheric structure across oblique continental collision in New Zealand from wide-angle *P* wave modeling, *J. Geophys. Res.*, *108*(B12), 2566, doi:10.1029/2002JB002286.

Sewell, R. J. (1988), Late Miocene volcanic stratigraphy of central Banks Peninsula, Canterbury, New Zealand, *N. Z. J. Geol. Geophys.*, *30*, 41–64.

Shelton, G., and J. A. Tullis (1981), Experimental flow laws for crustal rocks, *Eos Trans. AGU*, *62*, 396.

Sibson, R. H. (1982), Fault zone models, heat flow and the depth distribution of earthquakes in the continental crust of the United States, *Bull. Seismol. Soc. Am.*, *72*, 151–163.

Simpson, G. D. H., A. F. Cooper, and R. J. Norris (1994), Late Quaternary evolution of the Alpine Fault at Paringa, South Westland, New Zealand, *N. Z. J. Geol. Geophys.*, *37*, 49–58.

Stern, T. A., P. E. Wannamaker, D. Eberhart-Phillips, D. Okaya, J. F. Davey, and South Island Project Working Group (2001), Mountain building and active deformation studied in New Zealand, *Eos Trans. AGU*, *78*(32), 329, 335–336.

Sutherland, R. (1999), Cenozoic bending of New Zealand basement terranes and Alpine Fault displacement: A brief review, *N. Z. J. Geol. Geophys.*, *42*, 295–301.

Sutherland, R., P. King, and R. Wood (2001), Tectonic evolution of Cretaceous rift basins in south-eastern Australia and New Zealand: Implications for exploration risk assessment, in *Proceedings of Eastern Australasian Basins Symposium*, *Spec. Publ. AIMM*, edited by K. C. Hill and T. Bernecker, pp. 3–13, Pet. Explor. Soc. of Aust., Perth.

Templeton, A. S., D. Craw, P. O. Koons, and C. P. Chamberlain (1999), Near-surface expression of a young mesothermal gold mineralizing system, Sealy Range, Southern Alps, New Zealand, *Miner. Deposita*, *34*, 163–172, doi:10.1007/s001260050193.

Tindall, S. E., and G. H. Davis (1999), Monocline development by oblique-slip fault propagation folding: The East Kaibab monocline, Colorado Plateau, Utah, *J. Struct. Geol.*, *21*, 1303–1320, doi:10.1016/S0191-8141(99)00089-9.

Upton, P. (1998), Modelling localisation of deformation and fluid flow in a compressional orogen: Implications for the Southern Alps of New Zealand, *Am. J. Sci.*, *289*, 296–323.

Upton, P., and P. O. Koons (2007), Three-dimensional geodynamic framework for the central Southern Alps, New Zealand: Integrating geology, geophysics and mechanical observations, in *A Continental Plate Boundary: Tectonics at South Island, New Zealand, Geophys. Monogr. Ser.*, vol. 175, edited by D. Okaya, T. Stern, and F. Davey, pp. 255–272, AGU, Washington, D. C.

Upton, P., D. Craw, T. G. Caldwell, P. O. Koons, Z. James, P. E. Wannamaker, G. J. Jiracek, and C. P. Chamberlain (2003a), Upper crustal fluid flow in the outboard region of the Southern Alps, New Zealand, *Geofluids*, *3*, 1–12, doi:10.1046/j.1468-8123.2003.00046.x.

Upton, P., P. O. Koons, and D. Eberhart-Phillips (2003b), Extension and partitioning in an oblique subduction zone, New Zealand: Constraints from three-dimensional numerical modeling, *Tectonics*, *22*(6), 1068, doi:10.1029/2002TC001431.

Upton, P., D. Craw, Z. James, and P. O. Koons (2004), Structure and late Cenozoic tectonics of the Southern Two Thumb Range, mid-Canterbury, New Zealand, *N. Z. J. Geol. Geophys.*, *47*, 141–153.

Upton, P., M. Begbie, and D. Craw (2008), Numerical modelling of mechanical controls on coeval steep and shallow dipping auriferous quartz vein formation in a thrust zone, Macraes mine, New Zealand, *Miner. Deposita*, *43*, 23–35, doi:10.1007/s00126-007-0148-0.

Van Avendonk, H. J. A., W. S. Holbrook, D. Okaya, J. K. Austin, F. Davey, and T. Stern (2004), Continental crust under compression: A seismic refraction study of South Island Geophysical Transect I, South Island, New Zealand, *J. Geophys. Res.*, *109*, B06302, doi:10.1029/2003JB002790.

Wandres, A. M., and J. D. Bradshaw (2005), New Zealand tectonostratigraphy and implications from conglomeratic rocks for the configuration of the SW Pacific margin of Gondwana, in *Terrane Processes at the Margins of Gondwana*, edited by A. P. M. Vaughan, P. T. Leat, and J. J. Pankhurst, *Geol. Soc. Spec. Publ.*, vol. 246, pp. 179–216.

Wannamaker, P. E., G. R. Jiracek, J. A. Stodt, T. G. Caldwell, V. M. Gonzalez, J. D. McKnight, and

A. D. Porter (2002), Fluid generation and pathways beneath an active compressional orogen, the New Zealand Southern Alps, inferred from magnetotelluric data, *J. Geophys. Res.*, *107*(B6), 2117, doi:10.1029/2001JB000186.

Wellman, H. W. (1979), An uplift map of the South Island of New Zealand, and a model for uplift in the Southern Alps, in *Origin of the Southern Alps*, edited by R. I. Walcott and M. M. Cresswell, *Bull. R. Soc. N. Z.*, vol. 18, pp. 13–20.

Willett, S. C., C. Beaumont, and P. Fullsack (1993), Mechanical model for the tectonics of doubly vergent compressional orogens, *Geology*, *21*, 371–374, doi:10.1130/0091-7613(1993)021<0371:MMFTTO> 2.3.CO;2.

_____

D. Craw, Geology Department, University of Otago, P.O. Box 56, Dunedin 9054, New Zealand.

R. Enlow, Department of Mathematics and Statistics, University of Otago, P.O. Box 56, Dunedin 9054, New Zealand.

C. M. Henderson, Department of Geological Sciences, School of Geography, Environment and Earth Sciences, Victoria University, P.O. Box 600, Wellington 6140, New Zealand.

P. O. Koons, Department of Earth Sciences, University of Maine, Orono, ME 04469, USA.

P. Upton, GNS Science, Private Bag 1930, Dunedin, 9054, New Zealand. (p.upton@gns.cri.nz)